Indian Journal of Pure & Applied Physics
Vol. 55, January 2017, pp. 73-80

Electrophoretic deposition of plasmonic nanocomposite for the fabrication of dye-sensitized solar cells

Swati Bhardwaj[a], Arnab Pal[b], Kuntal Chatterjee[b], Papia Chowdhury[c], Susmita Saha[d], Anjan Barman[d], Tushar H Rana[a], Ganesh D Sharma[a]* & Subhayan Biswas[a]

[a]Department of Physics, The LNM Institute of Information Technology, Jaipur 302 031, India

[b]Vidyasagar University, Midnapore 721 102, India

[c]Jaypee Institute of Information Technology, Noida 201 307, India

[d]S N Bose National Centre for Basic Sciences, Kolkata 700 098, India

Received 30 August 2016; revised 1 November 2016; accepted 30 November 2016

TiO_2-Ag nanocomposites have been prepared by hydrothermal process for the preparation of photoelectrode for dye-sensitized solar cells. The formation of TiO_2-Ag nanocomposites have been confirmed by the transmission electron microscopy (TEM), UV-Vis spectroscopy, X-ray diffraction and energy dispersive X-ray analysis. The TEM images confirm that silver nanoparticles of average size 30 nm are dispersed inside the TiO_2 matrix. Electrophoretic deposition technique (EPD) is successfully utilized to incorporate TiO_2-Ag nanocomposites in commercially available TiO_2 nanoparticle to prepare photoelectrode on transparent oxide substrate. Incorporation of TiO_2-Ag nanocomposites by EPD technique has been done in different ways: in all the layers of TiO_2 photoelectrode and in only the top layer of TiO_2 photoelectrode. X-ray diffraction, field effect scanning electron microscopy in back scattered mode and photoluminescence (PL) spectroscopy study confirm the presence of TiO_2-Ag nanostructure in prepared photoelectrode. The current-voltage characteristic shows 78% and 67% enhancement of photocurrent and power conversion efficiency (PCE) respectively in the DSSC with Ag incorporated photoelectrode compared to the cell without Ag nanoparticles and maximum PCE obtained in DSSC with TiO_2-Ag is 7.5%.

Keywords: Dye sensitized solar cells, Plasmonic nanocomposite, Electrophoretic deposition

1 Introduction

Over the last two decades dye sensitized solar cell (DSSC) has emerged as one of the most important low cost solar cells in the domain of photovoltaic devices[1]. Although the rate of improvement of maximum power conversion efficiency (PCE)[2] achieved in DSSC is not very high, but stability[3] and affordability has been greatly enhanced in the last few years. In order to increase the PCE of DSSC, researcher focus on the improvement of individual components[4-9] of DSSC as well as on the interrelation of the components[10,11]. Certain modifications of TiO_2 photoelectrode, like the inclusion of scattering layer of bigger TiO_2 particles[12], $TiCl_4$ treatment of TiO_2 photo electrode[13], give an explicit improvement of solar cell performance and became a part of the routine fabrication process of DSSC. A novel method to increase the light absorption is the incorporation of metallic nanoparticles in the TiO_2 electrode[14,15] which improves the overall PCE of DSSCs[16-20]. The application of silver and gold nanoparticles decorated TiO_2 photoelectrode in DSSC improves the light absorption property as well as PCE in all the previous reported studies. The plasmonic nanoparticles act as an efficient light trapping in several ways which include far-field scattering, near-field localized surface plasmons (LSPs) and surface plasmon polaritons at the metal semiconductor interface[21]. Moreover, they play a major role as electron scavenger, which reduce electron-hole recombination and allow efficient electron transfer in DSSC[22]. The variation of shape, size and inter-particle space difference of plasmonic particles play important role in enhancing PCE of DSSC[10,23,24]. The preparation of silver or gold loaded photoelectrode can be classified into three broad categories: (i) preparation of nanocomposite of Ag or Au with TiO_2 followed by deposition of these nanocomposites on a transparent conducting substrate to prepare photoelectrode[25] (ii) decoration of TiO_2 nanostructures with Ag or Au nanoparticles by wet chemical technique[26] (iii) sophisticated physical deposition techniques to

*Corresponding author (E-mail: gdsharma273@gmail.com)

prepare Ag or Au-TiO_2nanocomposite photo electrode[27-29]. Among the chemical techniques, the process mentioned in the category is a superior technique than other two, where nanocomposite of TiO_2 and plasmonic particles can be tailor-made and later can be used for the photoelectrode deposition by doctor blade or spin coating technique. However, both 'doctorblade' technique as well as spin coating technique has their own limitations from the perspective of controlling structure and morphology of the resultant film and cannot be accomplished efficiently by the above mentioned techniques. On the other hand, layer by layer deposition of TiO_2 nanoparticles or composite of TiO_2 nanoparticles with plasmonic is not suitable by doctor blade technique. In the last two decades, Electrophoretic deposition EPD technique has gained a lot of attention due to its simple, low cost procedure and fast deposition rate[30]. EPD is a colloidal processing technique which utilizes external electric field for the deposition of thin film from charged suspended nanoparticles. EPD technique is suitable for layer by layer deposition of homogeneous porous metal oxide thin film on a transparent conducting oxide substrate. In the EPD technique, TiO_2 film is deposited from stable suspension of charged colloidal particles by the application of a dc electric field. There are two advantages of the charging of colloidal particles (i) columbic attraction permits the deposition on the oppositely charged electrode (ii) repulsion between the colloidal particles lead to the formation of stable suspension[31]. EPD has been successfully utilized for the preparation of TiO_2 photoelectrode of DSSC[31-37]. The study by Hsisheng's group revealed that the deposition of TiO_2 photoelectrode by EPD technique gives better performance than the same prepared by standard doctor blade technique[35,36]. It was found that the thickness of TiO_2 film increases with deposition time, deposition voltage[33]. Multilayer deposition in EPD technique is very effective in producing crack free TiO_2 photoelectrode[34]. Post deposition hydraulic pressure is also used to enhance connectivity between the TiO_2 particles[32]. EPD technique has been utilized for the deposition of different nanostructures of TiO_2 as well as composite materials, TiO_2/C[38]; SnO_2/TiO_2[39]; TiO_2 nanotube-WO_3[40]; TiO_2- carbon nanotube[41] for various applications. TiO_2-Ag has also been deposited on 3D nickel filter by EPD technique for the application as an anti-microbial material[42].

In this work, an effort has been made to incorporate silver nanoparticle in TiO_2 nano network to form a nanocomposite by hydrothermal technique. As the size of the hydrothermally prepared composite particle is ~200 nm, the motivation was that the mixing of these plasmonic composite particle with commercially available TiO_2 nanoparticles of the size~20nm may give an interesting result as there is a possibility that apart from its' plasmonic contribution, these bigger composite particles can also act as light scatters. Electrophorectic deposition (EPD) technique has been chosen to deposit plasmonic composites along with commercially available TiO_2 nanoparticles in layer by layer fashion on fluorine doped tin oxide (FTO) coated substrate for the application in DSSC. Incorporation of TiO_2-Ag nanocomposites by EPD technique has been done in two different ways: in all the layers of TiO_2 photoelectrode and in only the top layer of TiO_2 photoelectrode. The Ag incorporated TiO_2 the photoelectrode based DSSC has overall PCE of 7.5%.

2 Method and Materials

All the chemicals (analytical grade) used for the synthesis of Ag-TiO_2 nanocomposites were purchased from Merck. Here two solutions were prepared; one consists of 0.5 M silver nitrate ($AgNO_3$) used as precursor in 10 mL ethylene glycol. The solution was stirred for 20 min. Another solution contains TTIP (titanium tetraisopropoxide) of 2M in 10 mL ethyl alcohol (C_2H_5OH) was stirred for 15 min. Then the first solution was added drop wise in the later under vigorous stirring condition. The mixed solution, after stirring for another 15 min, was transferred in a Teflon autoclave with a stainless steel jacket and kept at 240° C for 14 h. The obtained product was cooled to room temperature and the precipitate was repeatedly washed and centrifuged and dried at 60° C. The dried powder was annealed at 500° C for 1 h for better crystallization of TiO_2 in the as required Ag-TiO_2 nanocomposite and used for thin film deposition. Thin film of TiO_2-Ag nanocomposites were deposited on FTO substrate along with commercially available TiO_2 using EPD technique. Highly pure TiO_2 nanoparticles with average size 25 nm, supplied from Sigma Aldrich (purity 99.9 %), were used for the deposition of all the photoelectrodes. The EPD was done from non-aqueous solution containing acetylacetone and iodine. Before the deposition, ultrasonication was done for 30 minutes as well as vigorous stirring for one hour at 5° C. The FTO (25 mm×25 mm×2 mm) substrate was first cleaned

with the acetone and then with isopropyl alcohol. Platinum foil (purity 99.9%) was used as a cathode. The schematic diagram of the EPD setup has been shown in Fig. 1(ii) (inset). The interspacing distance between the platinum and FTO coated glass electrode was kept at 35 mm. Anodic electrophoretic deposition was performed at room temperature at a constant voltage achieved through a source meter (Model-2400, Keithley Instrument Ins). The current response of the sample was monitored in real time. Initially, a constant voltage of 5 V was applied between the electrodes for 150 s, followed by deposition of four layers each of duration 20 s at 20 V. The applied voltage and duration are optimized values for the sample prepared with commercially available TiO_2 nanoparticles. Three samples were prepared with same deposition parameters: TiO_2 photoelectrode with commercially available TiO_2 nanoparticles (S1), using the precursor of TiO_2 (Aldrich) and TiO_2-Ag for only the top layer (S2), using the precursor of TiO_2 (Aldrich) and TiO_2-Ag for all the four layers (S3). The mass of deposited amount in S2 and S3 samples was kept equal to the S1 by slightly adjusting the duration of deposition. The samples were dried at room temperature and then annealed in nitrogen atmosphere at 450 °C. After annealing, all the samples were dipped in 40 mM of $TiCl_4$ for 1 h and calcined again at 450 °C in nitrogen atmosphere. A strong adhesion of TiO_2 film on FTO substrate was observed after annealing. The thickness of the thin films of TiO_2 was about 12-14 μm. All the photoelectrodes were soaked in N719 dye of concentration 0.5 mM in anhydrous ethanol for 24 h and washed with ethanol to remove the excess dye. The counter electrode was prepared by standard technique using choroplatinic acid (H_2PtCl_6). The DSSCs were fabricated by assembling photoelectrode and counter electrode using a sealant (Surlyn from Solaronix) of 60 μm thickness. The filling up of the electrolyte, composed of Acetonitrile, 0.1 M lithium iodide, 0.05 M iodine, 0.5 M 4-*tert* butylpyridine, and 0.6 M 1,2-dimethyl-3-propylimidazolium iodide (DMPII) was carried out through the holes, made on the counter electrode. The absorbance of the composite thin film of TiO_2 and silver nanoparticles (Ag) were obtained with the UV-Vis spectro photometer using an integrating sphere (ISR 240A) attachment. The current-voltage (*J-V*) measurements of DSSCs were performed by a Keithley 2400 unit with the help of the lab tracer under the source (AM 1.5, 100 mW/cm^2). Structural analysis of Ag–TiO_2 nanocomposite powdered samples were carried out by Rigaku Mini-Flex X-Ray diffractometer using Cu K_α radiation (λ = 1.54178 Å) source. Morphological analysis was done by both JEM 2100 transmission electron microscope at an accelerating voltage of 200 keV and FEI, inspect F scanning electron microscopy. EDAX was carried out in S-4200, Hitachi. The morphology and the structure of deposited samples were characterized by using field emission scanning electron microscopy (FESEM – JSM 7600F) and grazing incidence X ray diffraction (GIXRD-Panalytical Xpert Pro), respectively. Raman spectroscopy was carried out by Raman spectrometer equipped with a SPEX TRIAX 550 monochromator and a liquid-nitrogen-cooled charge-coupled device (CCD; Spectrum One with CCD 3000 controller, ISA JobinYovn). The typical spectral acquisition time was 1 min and spectral 76 resolutions chosen for Raman spectrum was 2 cm^{-1} in N_2 atmosphere. The PL

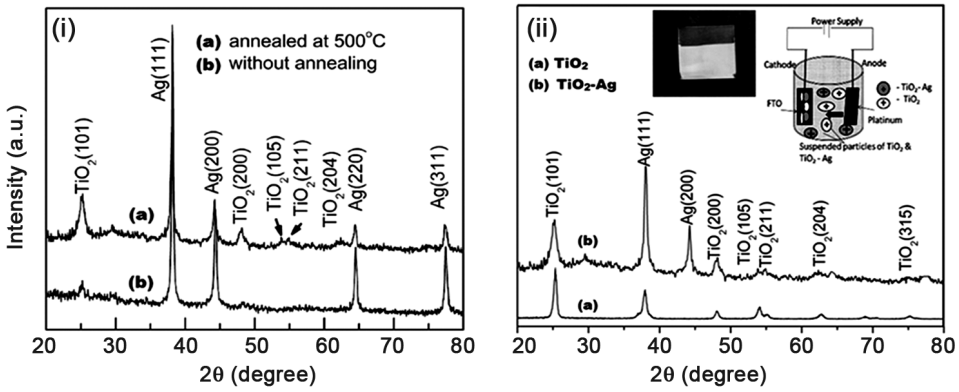

Fig. 1 — (i) The XRD patterns of the prepared TiO_2-Ag nanocomposite before and after annealing and (ii) (a) TiO_2 thin film (b) TiO_2-Ag incorporated TiO_2 thin film

spectra were recorded at 300 K with Perkin Elmer spectrophotometer (Model Fluorescence-55) by using 325 nm line of Xe lamp (Model LS 55 Series) as the excitation source at room temperature.

3 Results and Discussion

Figure 1 shows the XRD pattern of as-prepared and annealed sample of TiO_2-Ag nanocomposite. In the as-prepared powder sample the prominent diffraction peaks corresponding to the (111), (200), (220) and (311) plane of Ag nanoparticle are visible. The anatase phase of TiO_2, observed weakly in the as-prepared sample, has become prominent after annealing at 500 °C. No other phase of TiO_2 was observed. The particle size of Ag, calculated by the Debye-Scherrer technique and found to be 17.8 nm. The morphology of the as-prepared TiO_2-Ag nanocomposite was investigated by FESEM and TEM / HRTEM as shown in Fig. 2. The FESEM image indicates that Ag nanoparticles with particle size 20-40 nm are embedded in flake like TiO_2 matrix in an almost uniform manner. EDAX measurement also confirms the presence of Ag in 21.33 at% in the TiO_2-Ag composite. The TEM image exhibits Ag nanoparticles with darker shade which are spherical in nature, having a diameter between 20-40 nm and are embedded in the TiO_2 sheet. The HRTEM image shows that the nanocomposite particle has a good crystallinity and the measured inter planner distances confirm the (200) and (101) peak observed in the XRD pattern of Ag and TiO_2, respectively. The normalized UV–Vis absorption spectrum of the TiO_2-Ag nanocomposite film is shown in Fig. 3, shows sharp absorption edge of TiO_2 at 350 nm and exhibits characteristic[43] plasmon band at 428 nm. Surface plasmon band of a metal depends upon different factors, such as particle size, particle shape and the environment[10]. The inclusion of TiO_2-Ag nano-composites enhance the absorbance in the visible region. The energy bandgap of the prepared TiO_2-Ag nanocomposite has been calculated using the well known Tauc's plot method. The effective band gap observed (E_g = 2.96 eV) for this composite, shown in Fig. 3 (inset) is less than that of the TiO_2 semiconductor in anatase phase. The reduction in the band gap of the TiO_2-Ag nanocomposite as compared to anatase phase may be attributed to the free electron properties of Ag nanoparticles, which exhibited with a down shift in the conduction band and an upward shift in the valance band[44]. Hence incorporating the Ag NP into TiO_2 reduced the band gap and helped to extend the light absorption in the visible region. As shown in Fig. 3, the absorption has been broadened, might be due to the smaller size Ag nanoparticles.

Fig. 4(a) and (b) represent the images of FESEM recorded with back scattered electrons to identify the TiO_2-Ag from TiO_2. Since Ag has a higher atomic number, the TiO_2-Ag nano sheet is supposed to be brighter compared to TiO_2 nanoparticles. This image also shows the existence of such TiO_2-Ag nano composite on TiO_2 surface. The EDAX image of S1 and S2 sample also confirms the absence of any other impurities. The peak corresponding to Ag is not prominent, since at% of Ag in the S2 photo electrode is less than 1. The secondary FESEM image of the surface of S1 and S2 photo electrodes, shown in Fig. 4(c) and (d), exhibit homogeneous porous structure. It can be seen from these images that there is no apparent change in the morphology of the S1 after incorporation of TiO_2-Ag in S2. The use of low deposition applied voltage as

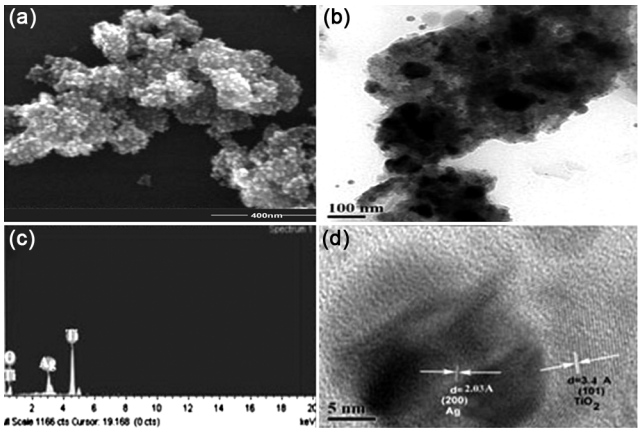

Fig. 2 — (Typical electron microscopy of TiO_2-Ag nanocomposite sample: (a) SEM (b) TEM (c) EDX and (d) HRTEM

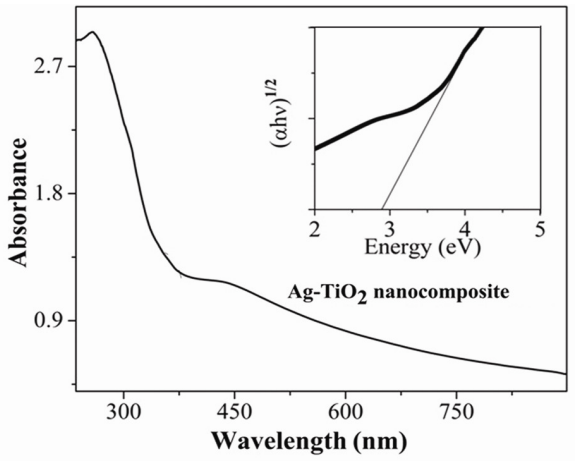

Fig. 3 — (Absorbance spectrum of TiO_2–Ag nanocomposite, (inset) Tauc plot of TiO_2–Ag nanocomposite

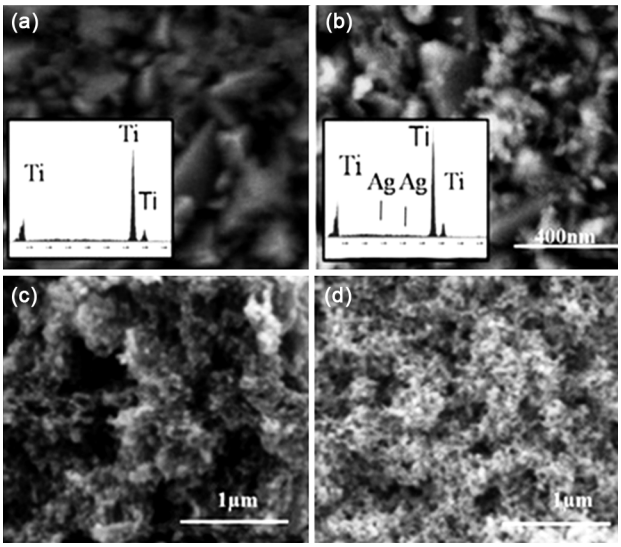

Fig. 4 — (Backscattered (BS) images and EDX images of TiO_2 thin film (a) without Ag (b) with Ag. Secondary SEM image of the top view of TiO_2 thin film (c) without Ag (d) with Ag

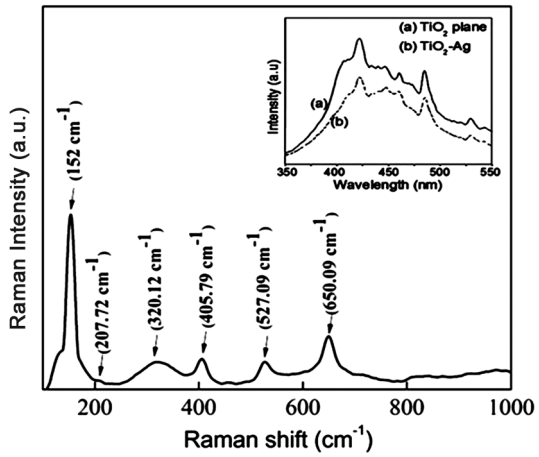

Fig. 5 — (Raman spectra of TiO_2-Ag with inset figure of photoluminescence spectra of annealed TiO_2 thin film photoelectrode (a) without TiO_2-Ag (b) with TiO_2-Ag. The excitation wavelength used in PL was λ_{exc}=290 nm

well as multiple coatings prevents the film from formation of micro cracks. The GIXRD of EPD deposited TiO_2 film (S1), depicted in Fig. 1(ii), shows anatase phase of TiO_2. The incorporation of Ag nanoparticles in the commercially available TiO_2 is confirmed by the XRD pattern of the TiO_2-Ag thin film sample (S2), which shows distinct diffraction peaks corresponding to the (111) and (200) plane of Ag nanoparticle. The particle size calculated from the XRD of the S2 sample is 17 nm, which is close to the value that has been obtained earlier for the powder TiO_2-Ag nanocomposite.

Understanding the charge recombination process occurring in the semiconductor is crucial for the photo-electrochemical properties and DSSC performance. The photoluminescence (PL) emission spectra of S1 and S2 thin film are shown in Fig. 5. The TiO_2 absorbs incident photons with sufficient energy equal to or higher than the band gap energy, but it produces photo induced charge carriers (h+--e-). The recombination of photo induced electrons and holes released in the form of PL. The PL intensity decreases with the incorporation of TiO_2-Ag nanocomposite in S1. The quenching of PL emission spectra of S1 due to incorporation of Ag in TiO_2 nanocomposite is mainly because the semiconductor Ag interface behaves like a Schottky barrier, which acts as an electron could sink to efficiently prevent electron-hole recombination[45]. Because of the Schottky barriers formed due to the built in potential between Ag and TiO_2 interface, the electrons are more easily swept towards the FTO instead of recombining with a hole in the electrolyte. The lower PL intensity for Ag-TiO_2 composite indicates less radiative charge recombination. No change in the peak position of the PL spectra of S2 from S1 indicates that there is no Ti-Ag bond formation. Raman spectroscopy has been used for phase identification of TiO_2-Ag nanocomposite. The raman spectrum, taken in the range 100 cm^{-1} to 1000 cm^{-1}, has been depicted in Fig. 5, which shows only TiO_2 anatase phase at 152, 208, 320, 517, and 650 cm^{-1}. Raman peak corresponding to Ag is absent due to very less amount of quantity present in the sample.

The effect of TiO_2-Ag nanocomposite on the optical property of the TiO_2 photoanode has been summarized in Fig. 6. The inset of Fig. 6(a) illustrates the absorbance of TiO_2-Ag nanocomposite which was measured inside an integrating sphere by diffuse transmittance mode. The Fig. 6(c) clearly shows the broad plasmonic peak at 415 nm, with FWHM of 90 nm. The slight deviation of plasmonic peak position from the bare TiO_2-Ag powder sample can be attributed to the fact that the surface plasmon band of a metal depends upon different factors, such as particle size, particle shape, surface charge density, dipole–dipole interaction[10]. A sample containing Ag nanoparticle with a small variation of shape and size can lead to a broad peak, which is a combination of multiple plasmonic peaks. The absorption spectra of N719 dye and N719 dye in the presence of TiO_2-Ag nanocomposite is shown in Fig. 6(a) and 6(b), respectively. The overall absorbance has increased in the entire visible and near infrared region. It has been

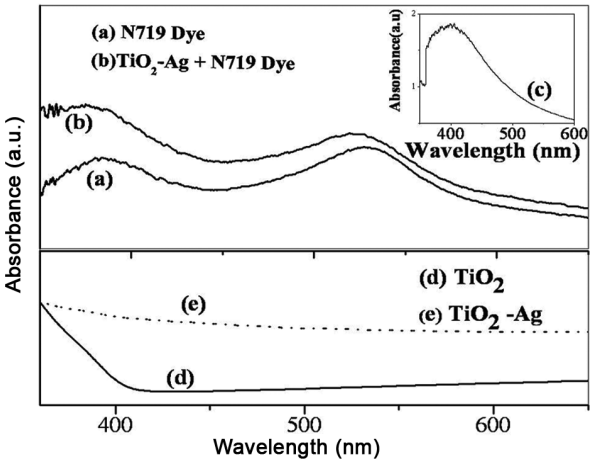

Fig. 6 — (Absorbance Spectra of (a) N719 dye (b) TiO_2-Ag nanocomposite with N719 Dye (c) TiO_2-Ag nanocomposite (d) TiO_2 thin film (e) TiO_2-Ag thin film

the absorption peak of the S2 sample has been shifted to lower wavelength 523 nm due to the presence of TiO_2-Ag nanocomposite, which can be attributed to the plasmonic effect of Ag. Figure 6(d) and 6(e) illustrate absorbance of S1 and S2, respectively, obtained from UV-Vis diffuse reflectance measurement. The absorbance spectrum of TiO_2 shows a characteristic band-edge below 400 nm with no absorbance in the visible range. The absorbance spectrum of S2 shows a significant amount of absorbance above 400 nm, which is due to localized surface plasmon resonance (LSPR) of Ag. Therefore, this can be attributed to the interaction of the molecular dipole in N719 with a strong localized electric field surrounding the Ag nanoparticles (NPs) in the thin film structure, as well as the possible additional enhancement of light scattering induced by AgNPs to prolong the optical path.

To investigate the effect of incorporation of TiO_2-Ag composite in TiO_2 photoelectrode we compared the performance of plasmonic DSSC (with photoelectrode S2 & S3) and standard DSSCs (with photoelectrode S1). The *J-V* characteristics of all the DSSCs under illumination are shown Fig. 7. The standard DSSC with photoelectrode S1 exhibits J_{SC} and V_{OC} 10.4 mA/cm^2 and 640 mV, respectively. These results are close to the reported values obtained in DSSC with photoelectrode TiO_2, prepared by EPD technique[35]. Both the plasmonic DSSC shows significant enhancement of $J_{SC,}$ i.e., 52% and 78% enhancement for the DSSC with photoelectrode S2 and S3, respectively, as compared to that for the standard DSSC.

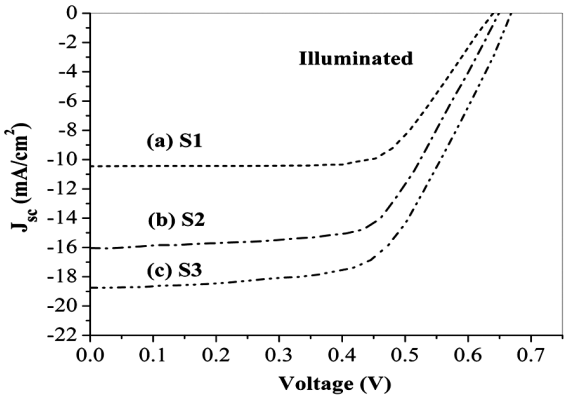

Fig. 7—(*J–V* characteristics of DSSC with the dye-sensitized photoelectrodes: (a) S1 (b) S2 (c) S3

Table 1—Photovoltaic performances DSSC with different photoelectrodes

Sample	J_{SC} (mA/cm^2)	V_{OC} (V)	*FF*	η (%)
S1	10.5	0.64	0.66	4.5
S2	16.0	0.65	0.61	6.4
S3	18.7	0.67	0.60	7.5

The V_{OC} of both the plasmonic DSSC is slightly higher than the standard DSSC with S1 photoelectrode. The fill factor (FF) and power conversion efficiency (PCE) of DSSC with photoelectrode S2 and S3 are 0.61 and 6.4 %, 0.61 and 0.60 and 7.5 %, respectively as shown in Table 1. The increase in the overall PCE is mainly due to the improvement in *Jsc*. Since the *Jsc* is related to the light harvesting efficiency of the photoanode. As mentioned above, the absorption has been improved for the Ag-TiO_2 composite as compared to TiO_2 and the absorption is mostly arises from the LSPR of Ag nanoparticles. This increase is a measure factor in boosting the absorption cross-section of dye molecules[46]. The plasmonic excitation strengthens the optical density of incident light near the surface of Ag nanoparticles. Due to the high porosity and large pore size, the Ag–TiO_2 micro-spheres provide a high internal surface area for dye adsorption in the interior of the micro-spheres[47] which is enhanced by strong coupling between the electronic transitions of the dye molecules and the locally enhanced electromagnetic fields of the Ag NPs. This consequently results in the dye molecules harvesting more photons. As mentioned previously, light scattering by TiO_2-Ag nanocomposite sheet of dimension 200-300 nm could be one of the reasons of this enhancement apart from plasmonic effect of metal nanoparticle. In S2 sample, 3.75 wt % of TiO_2-Ag nanocomposite was present. The use of larger TiO_2 particles deposited on top of

the mesoporous film increases the radiation path length within the film and improves in harvesting of long wavelength photons[48,49]. However, use of larger amount of bigger particle reduces the effective area, dye-loading and the overall performance of the DSSC[50]. Although the S3 sample contains 15 wt% of bigger particle (TiO_2-Ag composite), the DSSC with this photoelectrode shows further higher photovoltaic performance, which indicates that scattering by bigger particle is not the sole reason for this enhancement of photovoltaic performance. The S3 photoelectrode has more amount of Ag-loading since the nanocomposite has been incorporated in all the layers which are the main reason for the exhibition of superior photovoltaic property. Moreover, the LSPR effect of Ag NPs would extend the light scattering and motivating the photo generated carriers in the semiconductor by transferring the plasmonic energy from Ag to the TiO_2 semiconductor[51,52,53].

The V_{OC} of both the plasmonic DSSC is slightly higher than the standard DSSC with S1 photoelectrode. Small amount of enhancement of V_{OC} may be due to the fact that the Ag nanoparticles behave like an electron scavenger which contributes to shift of the Fermi level of the nanocomposite to more negative potential, which in turn enhance the V_{OC}[14]. The dark current of plasmonic solar cell with photoelectrode S2 (which hasn't been shown in the figure) shows a lower value than the standard DSSC sample, which can be attributed to lesser back electron transfer due to charge accumulation in Ag nanoparticles, since the dark current is a measure of the back electron recombination.

4 Conclusions

Nanocomposite of TiO_2-Ag was successfully prepared by hydrothermal synthesis technique. The electron microscopy confirmed that the Ag nanoparticles are embedded in the TiO_2 sheet-like structure. The facile EPD technique has been fruitfully employed for the controlled deposition of the desired materials onto the substrate for the electrode formation. Layer by layer deposition of film by EPD is a very fast process. The DSSC with plasmonic photo electrode shows remarkable improvement in photocurrent and PCE has been increased up to 7.5 %. The enhancement of photocurrent may be attributed to the surface plasmon resonance due to Ag nanoparticles in TiO_2 matrix, scattering effect of bigger TiO_2-Ag nanocomposites and plasmonic coupling effect. Small amount of enhancement of V_{OC} may be due to the fact that the Ag nanoparticles behave like electron scavengers which contribute to shift of the Fermi level of the composite. The EPD technique has been proved to be a very effective technique for layer by layer deposition of TiO_2 for the application in DSSC. The incorporation of semiconductor coated plasmonic particle in TiO_2 has shown a lot of promises in the field of DSSC and will open up scope for depositing plasmonic nanocomposites suitably in TiO_2 photoelectrode by the EPD technique.

Acknowledgment

This research is supported by the funding from CSIR scheme 03(1304)/13/EMR-II, UGC 42-1069/ 2013 (SR) and The LNM Institute of Information Technology, Jaipur.

References

1 Regan B O & Gratzel M, *Nature*, 353(1991) 737.
2 Meidan Y, *Mater Today*, 18 (2014) 155.
3 Jung H S & Lee J K, *Chem Phys Lett*, 4 (2013) 1682.
4 Kay A & Gratzel M, *Chem Mater*, 14 (2002) 2930.
5 Taguchi T, Zhang X, Sutanto I, Tokuhiro K, Rao T N, Watanabe H, Nakamori T, Uragamic M & Fujishima A, *Chem Commun*, 19 (2003) 2480.
6 Lee Y C & Hupp J T, *Langmuir*, 26 (2010) 3760.
7 Li T C, Spokoyny A M, Farha C X & Hup J T, *J Am Chem Soc*, 132 (2010) 4580.
8 Nattestad A, Mazor A K, Fisher M K R & U Batch, *Nat Mater*, 9 (2010) 31.
9 Li L, Gibson E A, Qin P, Boschloo G, Gorlov M, Hagfeldt A & Sun L, *Adv Mater,* 22 (2010) 1759.
10 Standridge S D, Schatz G C & Hupp J T, *J Am Chem Soc*, 131 (2009) 8407.
11 Jong N C, Prasittichai C & Hupp J T, *Langmuir*, 27 (2011) 14609.
12 Chou T P, Zhang Q, Russo B, Fryxell G E & Cao G, *J Phys Chem C*, 111 (2007) 6296.
13 Sommeling P M, Regan O B C, Haswell R R, Smit H J P, Bakker N J, Smits J J T, Kroon J M & Van Roosmalen J A M, *J Phys Chem B*, 110 (2006) 19191.
14 Choi H, Chen W Ta & Kamat P V, *ACS Nano*, 6 (2012) 4418.
15 Gangishetty M K, Lee K E, Scott R W J & Kelly T L, *ACS Appl Mater Interfaces*, 5 (2013) 11044.
16 Huang N, Chen F, Sun P, Sun X, Sebo B & Zhao X, *Electrochim Acta*, 143 (2014) 232.
17 Ng S P, Lu X, Ding N, Chi-Man L Wu & Lee C S, *Solar Energy*, 99 (2014) 115.
18 Dong H, Wu Z, Lu F, Gao Y, El-Shafei A, Jiao Bo, Ning S & Hou X, *Nano Energy*,10 (2014) 181.
19 Liu X H, Hou L X, Wang J F, Liu B, Yu Z S, Ma L Q, Yang S P & Fu G S, *Solar Energy*, 110 (2014) 627.
20 Dong H, Wu Z, Gao Y, El-Shafei A, Ning S Ya, Xi J, Jiao B & Hou X, *Org Elect*, 15 (2014) 2847.
21 Qi J, Dang X, Hammond P T & Belcher A M, *ACS Nano*, 5 (2011) 7108.

22 Zhao G, Kozuka H & Yoko T, *Solar Energy Mater Solar Cell,* 46 (1997) 219.
23 Ringe E, Zhang J, Langille M R, Sohn K, Cobley C M, Au L, Xia Y, Mirkin C A, Huang J & Marks L D, *Mater Res Soc Symp Proc*, 1208 (2010) 10.
24 Kawawaki T, Takahashi Y & TatsumaT, *J Phys Chem C*, 117 (2013) 5901.
25 Yun J, Hwang S H & Jang J, *ACS Appl Mater Interfaces*, **7** (2015) 2055.
26 Xiang L, Zhao X, Shang C & Yin J, *J Colloid Interface Sci*, 403 (2013) 22.
27 Song M K, Rai P, Ko K J, Jeon S H, Chon B S, Lee C H & Yu Y T, *RSC Adv*, 4 (2014) 3529.
28 Yen Y C, Chen H P, Chen J Z, Chen J A & LinK J, *ACS Appl Mate Interfaces,***7** (2015) 1892.
29 Sunaranmurthy A, Schuck P J, Conley N R & Moerner W E, *Nano Lett*, 6 (2006) 355.
30 Standridge S D, Schatz G C & Hupp J T, *J Am Chem Soc*,131 (2009) 8407.
31 Besra L & Liu M, *J Mater Sci Lett*, 52 (2007) 1.
32 Girinis L, Dor S, Ofir A & Zaban A, *J Photochem Photobiol A*, 198 (2008) 52.
33 Jarernboon W, Pimanpang S, Maensiri S, Swatsitang E & Amornkitbamrung V, *Thin Solid Films*, 517(2009) 4663.
34 Tan W, Yin X, Zhou X, Zhang J, Xiao X & Lin Y, *Electrochimica Acta*, 54 (2009) 4467.
35 Chiu W H, Lee K M & Hsieh W F, *J Power Sources*, 196 (2011) 3683.
36 Liou Y J, Hsiao P T, Chen L C, Chu Y Y &Teng H, *J Phys Chem C*, 115 (2011) 25580.
37 ChenL C, Hsieh C T, Lee Y L &Teng H, *ACS Appl Mater Intefaces*,5 (2013) 11958.
38 Narayan M R & Raturi A, *Int J Mater Eng Innov,* 3 (2012) 17.
39 Hernandez J M P, Manriquez J, Meas-Vong Y, F J Rodriguez & Chapman T W, *J Hazard Mater*,147 (2007) 588.
40 Zhou M, Yu J, Liu S, Zhai P & Jiang L, *J Hazard Mater*,154 (2008) 1141.
41 Park J H, Perk O & Kim S, *Appl Phys Lett*, 89 (2006) 163106.
42 Sun Y, Wang Y & Zhitomirsky I, *Colloids Surf A*, 418 (2013) 131.
43 Noberi C, Zaman A C, Üstünda C B, Kaya F & Kaya C, *Mater Lett*, 67 (2012) 113.
44 Wang X, Yu J C, Ho C & Mak A C, *Chem Comm*, 2262 (2005) DOI: 10.1039/B500605H.
45 Lim S P, Pandikumar A, Huang N M, Lim H N, Gu G & Ma T L, *RSC Adv*, 4 (2014) 48236.
46 Lim S P, Pandikumar A, Huang N M & Lim H N, *RSC Adv*, 4 (2014) 38111.
47 Chen B, Zhang W, Zhou X, Huang X, Zhao, Wang H, Liu M, Lu Y & Yang S, *Nano Energy*, 2 (2013) 906.
48 Ding Y, Zhou L, Mo L, Jiang L, Hu L, Li Z, Chen S & Dai S, *Adv Funct Mater*, 25 (2015) 5946.
49 Ito S, Chen P, Comte P, Nazeeruddin M K, Lisk P, Chy P Pe & Gratzel M, *Prog Photovoltaics*, 15(2007) 603.
50 Ghadir E, Taghavinia N, Zakeeruddin S M, Gratzel M & Moser J E, *Nano Lett*, 10 (2010) 1632.
51 Hamadaniana M, Sayahi H & Zolfagharici A R, *JNS*, 1 (2012) 139.
52 Garmaroudi Z A & Mohammadi M R*, J Am Ceram Soc*, 99 (2016) 167.
53 Danladi Eli, Gyuk P M, Ahmad M S, Baba G I & Sarki S H, *Int J Mater Sci Technol*, 5 (2016) 214.